Inorganic Chemistry
Article

Inorg. Chem. **2010**, *49*, 9191–9199 **9191**
DOI: 10.1021/ic100610t

Synthesis, Crystal Structure, and Photoluminescent Properties of Ternary Cd(II)/Triazolate/Chloride System

Gang Wei, Yu-Feng Shen, Yong-Ru Li, and Xiao-Chun Huang*

Department of Chemistry, Shantou University, Shantou, Guangdong Province, 515063 China

Received March 31, 2010

Solvothermal reactions of cadmium chloride and 1,2,4-triazole (Htrz) in different solvent mediums have successfully synthesized five ternary Cd(II)/trz/Cl^- complexes, $[Cd(trz)Cl]\cdot H_2O$ (**1**$\cdot H_2O$), $[Cd_4(trz)_5Cl_3(H_2O)]\cdot(THF)_{1.25}\cdot(H_2O)_{2.5}$ (**2**$\cdot$1.25THF$\cdot$2.5H_2O), $[Cd_3(trz)_2Cl(MeCN)]$ (**3**), $[Cd_3(trz)_4Cl_2]\cdot(H_2O)_{0.5}$ (**4**$\cdot$0.5H_2O), and $[Cd_4(trz)_6Cl_2\text{-}(H_2O)_{0.5}]\cdot(H_2O)_{3.5}$ (**5**$\cdot$3.5H_2O). All of these five coordination polymers have three-dimensional (3-D) structural features, which are constructed by distinct substructures including clusters, chains, rings, and even 3-D frameworks. In all cases, 1,2,4-triazolate adopts a $\mu_{1,2,4}$ bridging mode, and chloride ions display a μ_2, μ_3, μ_4 bridging mode, respectively, which makes the structural diversity in the assembling system, for example, μ_4-Cl and cadmium triazolate, build up an unprecedented tetranuclear cluster $[Cd_4(trz)_8Cl]^-$ in **2**. All of the materials exhibit intense blue fluorescent emission and high thermal stability, wherein **1** presents an interesting guest-responsive photoluminescent property.

Introduction

It has been well-known that five-membered heterocycles, such as pyrazole, imidazole, triazole, and tetrazole are some kind of the simplest organic ligands, and these ligands play a significant role in the recognition and the crystallization of metal centers into metal−organic frameworks (MOFs), while deprontonated as bridged ligands. Moreover, their intriguing architectures and properties are exhibiting versatile potential application, such as gas storage, magnetism, catalysis, optics, microelectronics, even biology, and so on.[1,2]

Among these azoles, 1,2,4-triazole and its derivatives shows its particular versatile coordination modes in the build-up of clusters and MOFs, such as terminal as well as $\mu_{1,2}$, $\mu_{2,4}$, $\mu_{1,2,4}$ bridging fashions, in which $\mu_{1,2,4}$ bridging mode would be generally displayed, while the ligand was deprontonated as a trz (Htrz = 1,2,4-triazole) anion.[3−7] In other words, triazolate with $\mu_{1,2,4}$ bridging mode could be used as a three-connected organic linker to form neutral

*Corresponding author. E-mail: xchuang@stu.edu.cn.

(1) (a) Haasnoot, J. G. *Coord. Chem. Rev.* **2000**, *200*, 131–185. (b) Klingele, M. H.; Brooker, S. *Coord. Chem. Rev.* **2003**, *241*, 119–132. (c) Beckman, U.; Brooker, S. *Coord. Chem. Rev.* **2003**, *245*, 17–29. (d) Klingele, J.; Dechert, S.; Meyer, F. *Coord. Chem. Rev.* **2009**, *253*, 2698–2714. (e) Huang, X.-C.; Zhang, J.-P.; Chen, X.-M. *J. Am. Chem. Soc.* **2004**, *126*, 13218–13219. (f) Zhang, J.-P.; Chen, X.-M. *Chem. Commun.* **2006**, 1684–1689. (g) Ouellette, W.; Yu, M. H.; O'Connor, C. J.; Hagrman, D.; Zubieta, J. *Angew. Chem., Int. Ed.* **2006**, *45*, 3497–3500. (h) Zhang, J.-P.; Horike, S.; Kitagawa, S. *Angew. Chem., Int. Ed.* **2007**, *46*, 889–892. (i) Férey, G. *Chem. Soc. Rev.* **2008**, *37*, 191–214. (j) Zhang, J.-P.; Huang, X.-C.; Chen, X.-M. *Chem. Soc. Rev.* **2009**, *38*, 2385–2396.

(2) (a) Tian, Y.-Q.; Cai, C.-X.; Ren, X.-M.; Duan, C.-Y.; Xu, Y.; Gao, S.; You, X.-Z. *Chem.—Eur. J.* **2003**, *9*, 5673–5685. (b) Huang, X.-C.; Lin, Y.-Y.; Zhang, J.-P.; Chen, X.-M. *Angew. Chem., Int. Ed.* **2006**, *45*, 1557–1559. (c) Zhang, X.-M.; Zhao, Y.-F.; Zhang, W.-X.; Chen, X.-M. *Adv. Mater.* **2007**, *19*, 2843–2846. (d) Xu, J.-Y.; Qiao, X.; Song, H,-B.; Yan, S.-P.; Liao, D.-Z.; Gao, S.; Journaux, Y.; Cano, J. *Chem. Commun.* **2008**, 6414–6416. (e) Zhang, J.-P.; Kitagawa, S. *J. Am. Chem. Soc.* **2008**, *130*, 6010–6017.

(3) (a) Antolini, L.; Fabretti, A. C.; Gatteschi, D.; Giusti, A.; Sessoli, R. *Inorg. Chem.* **1990**, *29*, 143–145. (b) Antolini, L.; Fabretti, A. C.; Gatteschi, D.; Giusti, A.; Sessoli, R. *Inorg. Chem.* **1991**, *30*, 4860–4863. (c) Mösch-Zanetti, N.-C.; Ferbinteanu, M.; Magull, J. *Eur. J. Inorg. Chem.* **2002**, 950–956. (d) Müler-Buschbaum, K.; Mokaddem, Y. *Chem. Commun.* **2006**, 1684–1689. (e) Park, H.; Krigsfeld, G.; Teat, S. J.; Parise, J. B. *Cryst. Growth Des.* **2007**, *7*, 1343–1349. (f) Zhao, Z.-G.; Zhang, J.; Wu, X.-Y.; Zhai, Q.-G.; Chen, L.-J.; Chen, S.-M.; Xie, Y.-M.; Lu, C.-Z. *CrystEngComm* **2008**, *10*, 273–275. (g) Zhang, R.-B.; Li, Z.-J.; Cheng, J.-K.; Qin, Y.-Y.; Zhang, J.; Yao, Y.-G. *Cryst. Growth Des.* **2008**, *8*, 2562–2573. (h) Zhang, R.-B.; Li, Z.-J.; Qin, Y.-Y.; Cheng, J.-K.; Zhang, J.; Yao, Y.-G. *Inorg. Chem.* **2008**, *47*, 4861–4876.

(4) (a) Zhang, J.-P.; Zheng, S.-L.; Huang, X.-C.; Chen, X.-M. *Angew. Chem., Int. Ed.* **2004**, *43*, 206–1209. (b) Zhang, J.-P.; Lin, Y.-Y.; Huang, X.-C.; Chen, X.-M. *J. Am. Chem. Soc.* **2005**, *127*, 5495–5506. (c) Zhang, J.-P.; Lin, Y.-Y.; Zhang, W.-X.; Chen, X.-M. *J. Am. Chem. Soc.* **2005**, *127*, 14162–14163. (d) Zhai, Q.-G.; Lu, C.-Z.; Chen, S.-M.; Xu, X.-J.; Yang, W.-B. *Cryst. Growth Des.* **2006**, *6*, 1393–1398. (e) Yang, C.; Wang, X.-P.; Omary, M. A. *J. Am. Chem. Soc.* **2007**, *129*, 15454–15455. (f) Zhang, J.-P.; Chen, X.-M. *J. Am. Chem. Soc.* **2008**, *130*, 6010–6017. (g) Zhang, J.-P.; Chen, X.-M. *J. Am. Chem. Soc.* **2009**, *131*, 5516–5521. (h) Yang, C.; Wang, X.-P.; Omary, M. A. *Angew. Chem., Int. Ed.* **2009**, *48*, 2500–2505.

(5) (a) Ferrer, S.; Lloret, F.; Bertomeu, I.; Alzuet, G.; Borrás, J.; García-Granda, S.; Liu-González, M.; Haasnoot, J. G. *Inorg. Chem.* **2002**, *41*, 5821–5830. (b) Su, C.-Y.; Goforth, A. M.; Smith, M. D.; Pellechia, P. J.; zur Loye, H.-C. *J. Am. Chem. Soc.* **2004**, *126*, 3576–3586. (c) Ding, B.; Yi, L.; Cheng, P.; Liao, D.-Z.; Yan, S.-P. *Inorg. Chem.* **2006**, *45*, 5799–5803. (d) Ouellette, W.; Hudson, B. S.; Zubieta, J. *Inorg. Chem.* **2007**, *46*, 4887–4904. (e) Ouellette, W.; Prosvirin, A.-V.; Valeich, J.; Dunbar, K. R.; Zubieta, J. *Inorg. Chem.* **2007**, *46*, 9067–9082. (f) Li, J.-R.; Yu, Q.; Sañudo, E. C.; Tao, Y.; Bu, X.-H. *Chem. Commun.* **2007**, 2602–2604. (g) Halder, G. J; Park, H.; Funk, R. J.; Chapman, K. W.; Engerer, L. K.; Geiser, U.; Schlueter, J. A. *Cryst. Growth Des.* **2009**, *9*, 3609–3614. (h) Zhu, A.-X.; Lin, J.-B.; Zhang, J.-P.; Chen, X.-M. *Inorg. Chem.* **2009**, *48*, 3882–3884.

(6) Huang, X.-C.; Luo, W.; Shen, Y.-F.; Lin, X.-J.; Li, D. *Chem. Commun.* **2008**, 3996–3997.

Published on Web 09/21/2010

high-dimensional MOFs. Some successful three-connected porous MOFs have been reported for binary M(I)/triazolate systems, for example, trigonal coordinated Cu(I)/Ag(I) and trz in a ratio of 1:1 could assemble into a two-dimensional (6,3) network, and if decorating trz with some substituents, such as methyl, ethyl or amino etc., various three-connected three-dimensional porous frameworks could be obtained.[4] As compared to the M(I)/trz system, M(II)/trz system could hardly give a predictable topological network because of a flexible coordination geometry and a higher coordination number of M(II) ions, such as Cu(II), Zn(II), and Cd(II), etc., in addition, the higher positive valence usually needs other anion to meet the charge balance requirement.[5] One more anionic component, and even two or three kinds of other anions, was involved in most of the reported bivalent metal triazolates, which undoubtedly introduced inconstant factors into the reaction system to result in more uncertain products or mixtures. Recently, we reported a nanotubular architecture built from trinuclear $[Cu_3(trz)_2(\mu_3\text{-}O)(\mu\text{-}OH)]$ second building units (SBUs) and charge balance required anions (chloride and cyanurate).[6] In order to develop a profound understanding of the interaction between triazole and bivalent metal ions, we choose a ternary Cd(II)/triazolate/chloride system to further research on the internal relations of them. Considering the flexibility of Cd(II) coordination geometry and the versatility of triazolate binding modes, it is expected to find more different Cd−trz clusters as secondary building units (SBUs) in MOFs of the tenary M(II)/trz/chloride system.[7] These structurally diverse SBUs might provide wide possibilities for the construction of polymeric architectures.

In this study, we investigated the coordination ability of triazolate ligand with cadmium chloride and synthesized a series of coordination polymers, namely, $[Cd(trz)Cl\cdot H_2O]$ ($\mathbf{1}\cdot H_2O$), $[Cd_4(trz)_5Cl_3(H_2O)]\cdot(THF)_{1.25}\cdot(H_2O)_{2.5}$ ($\mathbf{2}\cdot$1.25-$THF\cdot 2.5H_2O$), $[Cd_3(trz)_2Cl(MeCN)]$ (**3**), $[Cd_3(trz)_4Cl_2]\cdot(H_2O)_{0.5}$ ($\mathbf{4}\cdot 0.5H_2O$), and $[Cd_4(trz)_6Cl_2(H_2O)_{0.5}]\cdot(H_2O)_{3.5}$ ($\mathbf{5}\cdot 3.5H_2O$). X-ray analyses exhibit that all of these complexes display interesting three-dimensional (3-D) frameworks with different novel topologies. The unusual structure, topologies, fluorescent properties, and thermal stability were described and discussed in detail.

Experimental Section

General Considerations. The following chemicals and solvents were obtained from commercial sources and used without further purification: cadmium chloride hemipentahydrate ($CdCl_2\cdot 2.5H_2O$), acetonitrile (MeCN), tetrahydrofuran (THF), pyridine, and 1,2,4-triazole (Htrz). *N*,*N*′-diformylhydrazine (DFH) was prepared according to the literature method.[8] Fluorescence spectra were measured on an Edinburgh Analytical instrument FLS920. Infrared spectra were recorded on a Nicolet Avatar 360 FTIR spectrometer in the range of 4000−400 cm^{-1} (KBr pellets). Elemental analyses (C, H, N) were performed with a Vario EL elemental analyzer. The phase purity of each product was checked by powder X-ray diffraction (PXRD) using a Rigaku D/M-2200T automated diffractometer. The observed and simulated powder XRD patterns of all complexes are displayed in Figure 8 and Figure S4, Supporting Information. Thermogravimetric analyses (TGA) were carried out on a Netzsch STA 449C equipment under nitrogen gas flow (40−800 °C range) at a heating rate of 10 °C·min^{-1}.

Synthesis of $[Cd(trz)Cl]\cdot H_2O$ ($\mathbf{1}\cdot H_2O$). A solution of $CdCl_2\cdot 2.5H_2O$ (0.5 mmol, 0.1140 g), Htrz (0.5 mmol, 0.0350 g), DFH (0.5 mmol, 0.0440 g), H_2O (4.0 mL), and THF (4.0 mL) was stirred for 15 min before heating to 140 °C in a 15 mL capacity Teflon-lined reaction vessel for 3 days under autogenous pressure, and then the reactant mixture was cooled at a rate of 0.1 °C min^{-1} to form colorless column crystals of $\mathbf{1}\cdot H_2O$, Yield: 80%. Elemental analysis calcd (%) for $C_2H_4N_3ClOCd$: C, 10.27; H, 1.72; N, 17.96. Found: C, 10.23; H, 1.81; N, 17.92. IR (solid KBr pellets, cm^{-1}): 3448 (s), 1654 (w), 1506 (s), 1290 (m), 1156 (s), 1068 (m), 1016 (w), 989 (m), 895 (w), 667 (m).

Synthesis of $[Cd_4(trz)_5Cl_3(H_2O)]\cdot 1.25THF\cdot 2.5H_2O$ ($\mathbf{2}\cdot$1.25-$THF\cdot 2.5H_2O$). A solution of $CdCl_2\cdot 2.5H_2O$ (0.5 mmol, 0.1140 g), Htrz (0.5 mmol, 0.0350 g), DFH (0.5 mmol, 0.0440 g), H_2O (2.0 mL), and THF (6.0 mL) was stirred for 15 min before heating to 160 °C in a 15 mL capacity Teflon-lined reaction vessel for 3 days under autogenous pressure, and then the reactant mixture was cooled at a rate of 0.1 °C min^{-1} to form colorless polyhedron crystals. Yield: 62%. Elemental analysis calcd (%) for $C_{15}H_{27}N_{15}Cl_3O_{4.75}Cd_4$: C, 17.17; H, 2.59; N, 20.02. Found: C, 17.21; H, 2.67; N, 19.98. IR (solid KBr pellets, cm^{-1}): 3384 (s), 1677 (w), 1503 (s), 1282 (m), 1158 (s), 1065 (m), 1045 (w), 991 (m), 880 (w), 665 (s), 544 (w).

Synthesis of $[Cd_3(trz)_2Cl(MeCN)]$ (3). A mixture of $CdCl_2\cdot 2.5H_2O$ (0.2 mmol, 0.0456 g), Htrz (0.2 mmol, 0.0140 g), DFH (0.2 mmol, 0.0176 g), H_2O (4.0 mL), and MeCN (4.0 mL) was heated at 160 °C in a 15 mL capacity Teflon-lined reaction vessel for 3 days under autogenous pressure. The mixture was cooled to room temperature at a rate of 0.1 °C min^{-1}. Colorless polyhedron crystals were isolated in 42% yield, washed with H_2O, and air dried. Elemental analysis calcd (%) for $C_6H_7N_7ClCd_3$: C, 13.10; H, 1.28; N, 17.83. Found: C, 13.05; H, 1.23; N, 17.91. IR (solid KBr pellets, cm^{-1}): 3436 (s), 1623 (w), 1495 (s), 1272 (m), 1197 (w), 1150 (s), 1166 (s), 987 (m), 875 (w), 669 (m), 471 (w).

Synthesis of $[Cd_3(trz)_4Cl_2]\cdot 0.5H_2O$ ($\mathbf{4}\cdot 0.5H_2O$). A mixture of $CdCl_2\cdot 2.5H_2O$ (0.2 mmol, 0.0456 g), Htrz (0.2 mmol, 0.0140 g), DFH (0.2 mmol, 0.0176 g), H_2O (2.0 mL), and MeCN (6.0 mL) was heated at 160 °C in a 15 mL capacity Teflon-lined reaction vessel for 3 days under autogenous pressure. The mixture was cooled to room temperature at a rate of 0.1 °C min^{-1}. Colorless polyhedron crystals were isolated in 45% yield, washed with H_2O, and air dried. Elemental analysis calcd (%) for $C_8H_9N_{12}Cl_2O_{0.5}Cd_3$: C, 13.94; H, 1.31; N, 24.38. Found: C, 13.91; H, 1.39; N, 24.32. IR (solid KBr pellets, cm^{-1}): 3466 (s), 1619 (m), 1495 (s), 1273 (m), 1194 (w), 1151 (s), 1067 (s), 990 (m), 869 (w), 670 (m), 467 (w).

Synthesis of $[Cd_4(trz)_6Cl_2(H_2O)_{0.5}]\cdot 3.5H_2O$ ($\mathbf{5}\cdot 3.5H_2O$). A solution of $CdCl_2\cdot 2.5H_2O$ (0.5 mmol, 0.1140 g), Htrz (0.5 mmol, 0.0350 g), DFH (0.5 mmol, 0.0440 g), H_2O (9.0 mL), and pyridine (1.0 mL) was stirred for 15 min before heating to 160 °C in a 15 mL capacity Teflon-lined reaction vessel for 3 days under autogenous pressure, and then the reactant mixture was cooled at a rate of 0.1 °C min^{-1} to form colorless polyhedron crystals. Yield: 22%. Elemental analysis calcd (%) for $C_{12}H_{20}N_{18}Cl_2O_4Cd_4$: C, 14.40; H, 2.01; N, 25.19. Found: C, 14.32; H, 1.95; N, 25.22. IR (solid KBr pellets, cm^{-1}): 3448 (s), 1637 (w), 1499 (s), 1276 (m), 1156 (s), 1067 (m), 985 (w), 872 (w), 669 (m).

(7) (a) Yi, L.; Ding, B.; Zhao, B.; Cheng, P.; Liao, D.-Z.; Yan, S.-P.; Jiang, Z.-H. *Inorg. Chem.* **2004**, *43*, 33–43. (b) Zhai, Q.-G.; Wu, X.-Y.; Chen, S.-M.; Lu, C.-Z.; Yang, W.-B. *Cryst. Growth Des.* **2006**, *6*, 2126–2135. (c) Ouellette, W.; Galón-Mascarós, J. R.; Dunbar, K. R.; Zubieta, J. *Inorg. Chem.* **2006**, *45*, 1909–1911. (d) Ouellette, W.; Prosvirin, A. V.; Chieffo, V.; Dunbar, K. R.; Hudson, B.; Zubieta, J. *Inorg. Chem.* **2006**, *45*, 9346–9366. (e) Zhai, Q.-G.; Lu, C.-Z.; Wu, X.-Y.; Batten, S.-R. *Cryst. Growth Des.* **2007**, *7*, 2332–2342. (f) Chen, S.-P.; Sun, S.; Gao, S.-L. *J. Solid State Chem.* **2008**, *181*, 3308–3316.

(8) (a) Wiley, R. H.; Hart, A. J. *J. Org. Chem.* **1953**, *18*, 1368–1371. (b) Ainsworth, C.; Jones, R. G. *J. Org. Chem.* **1954**, *77*, 622–624.

Table 1. Crystal Data and Structure Refinement for Complexes **1**−**5**

	1	**2**	**3**	**4**	**5**
formula	$C_2H_2N_3ClCd$	$C_{10}H_{12}N_{15}Cl_3OCd_4$	$C_{12}H_{13}N_{16}ClCd_3$	$C_{16}H_{18}N_{24}Cl_4OCd_6$	$C_{24}H_{26}N_{36}Cl_4OCd_8$
FW	215.92	914.30	754.06	1378.74	1875.80
space group	$P6_522$	$C2/m$	$Cmc2_1$	$Pnma$	$C2/c$
a (Å)	11.4544 (3)	26.8045(7)	10.3417(12)	16.9117(5)	20.6990 (8)
b (Å)	11.4544 (3)	11.0726(3)	33.579(4)	8.3292(3)	16.4603 (6)
c (Å)	11.1530(6)	10.8491(3)	13.4148(15)	13.0995(4)	18.0284 (7)
β (°)	90	109.5470(4)	90	90	118.089 (1)
V (Å^3)	1267.26(8)	3034.39(14)	4658.5(9)	1845.21 (10)	5419.0(4)
Z	6	4	8	2	4
T (K)	294(2)	294(2)	273(2)	294(2)	294(2)
D_{calcd} (g.cm^{-3})	1.698	2.001	2.150	2.482	2.299
R_{int}	0.0319	0.0163	0.0164	0.0184	0.0226
GOF	1.116	1.079	1.045	1.060	1.070
R_1[a] $[I > 2\sigma(I)]$	0.0126	0.0184	0.0217	0.0222	0.0222
wR_2[b] (all data)	0.0327	0.0489	0.0608	0.0581	0.0610
max, min peaks (e Å^{-3})	0.203,-0.223	0.361, −0.681	0.962, −0.868	0.921, −0.752	0.568, −1.666

[a] $R_1 = \sum|F_o| - |F_c||/\sum|F_o|$. [b] For all data, $wR_2 = \{[\sum w(F_o^2 - F_c^2)^2]/\sum[w(F_o^2)^2]\}^{1/2}$; $w = 1/[\sigma^2(F_o^2) + (aP)^2 + bP]$, where $P = [\max(F_o^2,0) + 2F_c^2]/3$.

Table 2. Summary of the Structural Characteristics of the Compounds of This Study and Related Materials

compd	dimensionality	coord geometry[a]	Cd−N	Cd−Cl	substructures
[Cd(trz)Cl] (**1**)	3-D	trig bipy, $\{N_3Cl_2\}$	2.221(2)−2.253(2)	2.6332(4)	$[Cd(trz)Cl]_n$ chains
$[Cd_4(trz)_5Cl_3(H_2O)]$ (**2**)	3-D	oct, $\{N_5Cl_1\}$	2.322(3)−2.359(4)	2.7424(3)	$[Cd_4(trz)_8Cl]^-$ clusters
		$\{N_4Cl_2\}$	2.309(3)−2.322(3)	2.6763(4)−2.8600(4)	$[Cd_2(trz)Cl]^{2+}$ clusters
		trig bipy, $\{N_3ClO\}$	2.219(3)−2.260(3)	2.618(9)−2.6193(8)	
$[Cd_3(trz)_2Cl(MeCN)]$ (**3**)	3-D	oct, $\{N_5N_{1(MeCN)}\}$	2.301(3)−2.345(4)		$[Cd_3(trz)Cl_2]_n^{3n+}$ chains
		(×2)	2.302(3)−2.322(3)	2.692(2)	$[Cd_6(trz)_6]^{6+}$ rings
		$\{N_5Cl_1\}$	2.335(3)−2.394(5),	2.675(2)	
		(×2)	2.309(3)−2.445(5)	2.640(2)−2.689(1)	
		$\{N_4Cl_2\}$	2.303(3)−2.317(3)		
		$\{N_6\}$	2.315(3)−2.505(4)		
$[Cd_3(trz)_4Cl_2]$ (**4**)	3-D	oct, $\{N_4Cl_2\}$	2.302(2)−2.354(2)	2.6493(6)−2.7227(6)	$[Cd_3Cl_2]_n^{4n+}$ chains
		trig bipy, $\{N_4Cl\}$	2.228(3)−2.357(3)	2.6648(9)	$[Cd(trz)_2]_n$ layer
$[Cd_4(trz)_6Cl_2(H_2O)_{0.5}]$ (**5**)	3-D	oct, $\{N_5Cl\}$	2.316(3)−2.381(3)	2.7764(9)	$[Cd_5(trz)_8Cl_4]_n^{2n-}$ layers
		$\{N_4Cl_2\}$	2.289(3)−2.373(3)	2.688(1)−2.8600(4)	$[Cd_3(trz)_4]_n^{2n+}$ chains
		(×2)	2.298(3)−2.325(3),	2.682(1)	
		$\{N_4ClO\}$,	2.258(3)−2.402(3)	2.7497(9)	
		$\{N_6\}$	2.327(3)−2.383(3)		
$[Cd_2(trz)_2Cl_2(H_2O)]$[3d]	3-D	oct, $\{N_4Cl_2\}$ and	2.303(2)−2.306(2)	2.6743(8)−2.6830(8)	$[Cd(trz)_2Cl]_n^{n-}$ chains
		$\{N_2Cl_3O\}$	2.217(2)	2.7090(8)−2.7406(8)	$[Cd(trz)_2Cl_2]_n^{2n-}$ chains

[a] Key: trig bipy, trigonal bipyramidal; and oct, octahedral.

X-ray Crystallography. All single crystals of these five reported complexes were carefully selected under an optical microscope and glued to thin glass fibers. Structural measurements were performed on a computer-controlled Siemens Smart CCD diffractometer with graphite-monochromated Mo Kα radiation (λ = 0.71073 Å) at 294 K. Absorption corrections were applied by using the multiscan program SADABS.[9a] Structural solutions and full-matrix least-squares refinements based on F^2 were performed with the SHELXS-97 program packages,[9b] respectively. Anisotropic thermal parameters were applied to all nonhydrogen atoms. All the hydrogen atoms were generated geometrically. In $\mathbf{1}\cdot H_2O$, $\mathbf{2}\cdot 1.25THF\cdot 2.5H_2O$, and $\mathbf{5}\cdot 3.5H_2O$, the highly disordered solvent molecules could not be satisfactorily modeled, so they were removed from the atom list for refinement and the PLATON/SQUEEZE procedure was applied.[9c] Crystal data as well as details of data collection and refinements for the complexes are summarized in Table 1. Atomic positional parameters, full tables of bond lengths and angles, and anisotropic temperature factors are available in the Supporting Information. Selected structural characteristics are given in Table 2.

(9) (a) Sheldrick, G. M. *SHELXL97, Program for Crystal Structure Refinement*; University of Göttingen: Göttingen, Germany, 1997. (b) Sheldrick, G. M. *SHELXS97, Program for Crystal Structure Solution*; University of Göttingen: Göttingen, Germany, 1997. (c) Spek, A. L. *J. Appl. Crystallogr.* **2003**, *36*, 7–13.

Results and Discussion

Syntheses, Infrared Spectroscopy, and X- Ray Power Diffraction. The hydrothermal reaction has provided a convenient method for the preparation of single crystals of inorganic−organic hybrid materials. The product composition may depend on critical factors, such as pH value of the reaction medium and temperature, especially the charge balancing anionic component which may also be incorporated into the final product. In the series of materials described in this contribution, charge-balancing chloride ions are incorporated in all cases, wherein chloride ions display dramatically different coordination modes, such as μ_2-, μ_3-, and even μ_4-bridging. On the other hand, all of triazolates in these five coordination polymers are ligated to cadmium atoms in $\mu_{1,2,4}$ bridging fashion. The complexes of this study were prepared in modest to good yields by exploiting the hydrothermal reactions of 1,2,4-triazole with $CdCl_2\cdot 2.5H_2O$ at 160 °C for 72 h, and the adjustment of the reaction temperature as well as the reaction time could not give more satisfactory products. Through systematic investigation to the reaction conditions we found that the ternary Cd(II)/trz/Cl system is remarkably sensitive to the reaction medium, while the

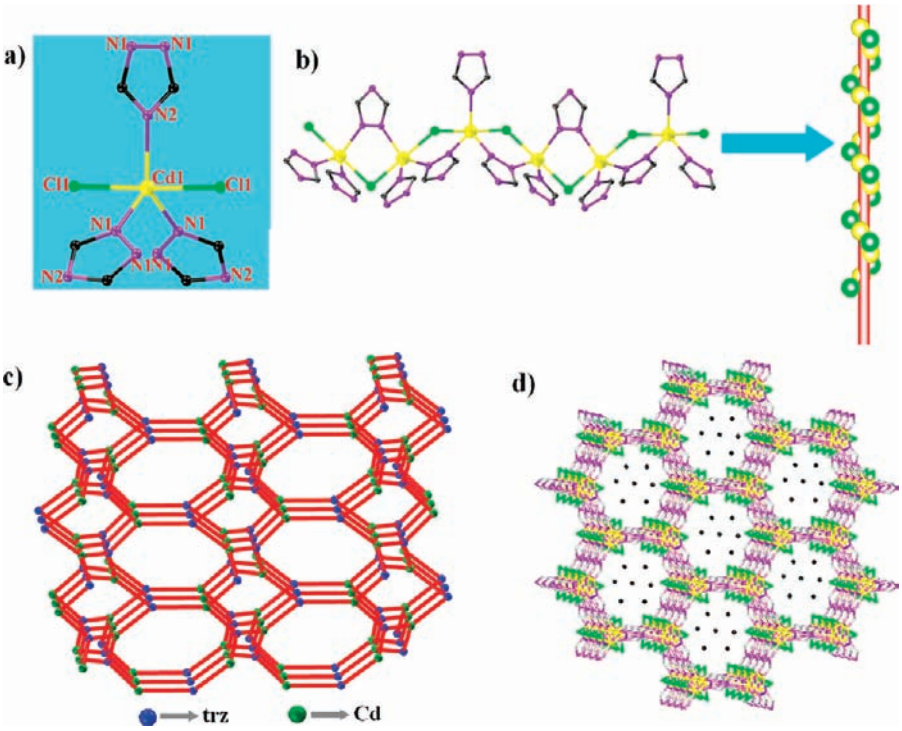

Figure 1. (a) View of the coordination environment of cadmium atom in **1**. (b) View of $[Cd(trz)Cl]_n$ chain substructure and the left-handed 3_1 helical chain in **1**. (c) Schematic representation of 3-D three-connected uniform (8, 3) topology network in **1**. (d)The 3-D structure of **1**, showing the large channels.

different ratio of $CdCl_2$ and Htrz had little effect on the final outcome. As compared to the common ratio of 1:1 for Cd(II):trz used in the syntheses of the above complexes, the results gave different ratios of 1:1, 4:5, 3:2, 3:4, and 2:3 for complexes **1**−**5**, respectively. The key to successful preparation of diverse products from the same origin is the control of the mixed solvent component. For example, the reaction of $CdCl_2 \cdot 2.5H_2O$ and Htrz in H_2O and THF following the volume ratio of 1:1 and 1:3 would yield $[Cd(trz)Cl] \cdot H_2O$ (**1**$\cdot H_2O$) and $[Cd_4(trz)_5Cl_3(H_2O)] \cdot (THF)_{1.25} \cdot (H_2O)_{2.5}$ (**2**$\cdot 1.25THF \cdot 2.5H_2O$), respectively, and while in the H_2O/MeCN medium, $[Cd_3(trz)_2Cl(MeCN)]$ (**3**) and $[Cd_3(trz)_4Cl_2] \cdot (H_2O)_{0.5}$ (**4**$\cdot 0.5H_2O$) could be obtained in the volume ratio of 1:1 and ca. 1:3, respectively. Finally, when the reaction was carried out in H_2O/pyridine at the ratio of 9:1, only $[Cd_4(trz)_6Cl_2(H_2O)_{0.5}] \cdot (H_2O)_{3.5}$ (**5**$\cdot 3.5H_2O$) was observed. It should be mentioned that the basicity of the reaction medium was adjusted through the addition of DFH in all the situations, which is the best reagent for the syntheses of this ternary system other than inorganic or organic bases, such as ammonia, pyridine, DMF, etc.

The IR spectra of **1**−**5** are characterized by a series of medium-to-strong intensity bands in the 660−1525 cm^{-1} range, the most prominent of which are four bands in the ranges of 1490−1525, 1270−1290, 1150−1165, and 660−670 cm^{-1}, associated with ν(C−H), ν(C−N), or ν(N−N) of the triazolate ligand vibrations. All of complexes except for **3** exhibit a strong broad band at ca. 3400−3450 cm^{-1}, which could be attributed to ν(O−H) of the lattice water molecules.

The purity of the complexes can be convincingly established by X-ray powder diffraction measurements. (Patterns for all of complexes can be found in Figure 8 and Figure S4, Supporting Information). It is clear that the observed patterns closely match the as-synthesized ones.

Structure Description. The exclusive crystallographically independent cadmium atom in [Cd(trz)Cl] (**1**) adopts trigonal bipyramidal $\{N_3Cl_2\}$ coordination geometry with three nitrogen atoms from three trzs in the equatorial plane and two axial chlorine atoms (Figure 1a). The crystallographically independent chlorine atom bridges two cadmium atoms to extend along the *b*-axis to be a left-handed 3_1 helical chain, as shown in Figure 1b. As far as we know, for the ternary metal/trz/halide system, no helical structures which have chloride composition were reported prior to our study, although rare chiral lattices were observed.[10]

Furthermore, as shown in Figure 1c, if we consider both the trz and Cd(II) as three-connected nodes, the 3-D framework exhibits a noninterpenetrated uninodal three-connected net, which can be presented as an eta network topology with the Schläfli symbol 8^3 and a long vertex symbol $8.8.8^2$.[5h,11] The most fascinating aspect of this structure is that the chiral network is built from achiral components.

This 3-D open framework is isostructural to the reported complex [Zn(trz)F] with a different metal center and anion and gives larger parallel open honeycomb channels than [Zn(trz)F] (Figure 1d).[5d,12] The hexagonal channels in **1** have a size of approximately 9.7 Å in diameter, which are occupied by the lattice water

(10) (a) Masood, M. A.; Enemark, E. J.; Stack, T. D. P. *Angew. Chem., Int. Ed.* **1998**, *37*, 928–932. (b) Mizukami, S.; Houjou, H.; Nagawa, Y.; Kanesato, M. *Chem. Commun.* **2003**, 1148–1149. (c) Chen, X.-Y.; Shi, W.; Xia, J.; Cheng, P.; Zhao, B.; Song, H.-B.; Wang, H.-G.; Yan, S.-P.; Liao, D.-Z.; Jiang, Z.-H. *Inorg. Chem.* **2005**, *44*, 4263–4269.

(11) (a) Batten, S. R.; Robson, R. *Angew. Chem., Int.Ed.* **1998**, *37*, 1460–1494. (b) Wu, T.; Yi, B.-H.; Li, D. *Inorg. Chem.* **2005**, *44*, 4130–4132. (c) Li, J.-R.; Tao, Y.; Yu, Q.; Bu, X.-H.; Sakamoto, H.; Kitagawa, S. *Chem.—Eur. J.* **2008**, *14*, 2771–2776.

(12) Goforth, A. M.; Su, C.-Y.; Mipp, R.; Macquart, R. B.; Smith, M. D.; Zur Loye, H.-C. *J. Solid State Chem.* **2005**, *178*, 2511–2518.

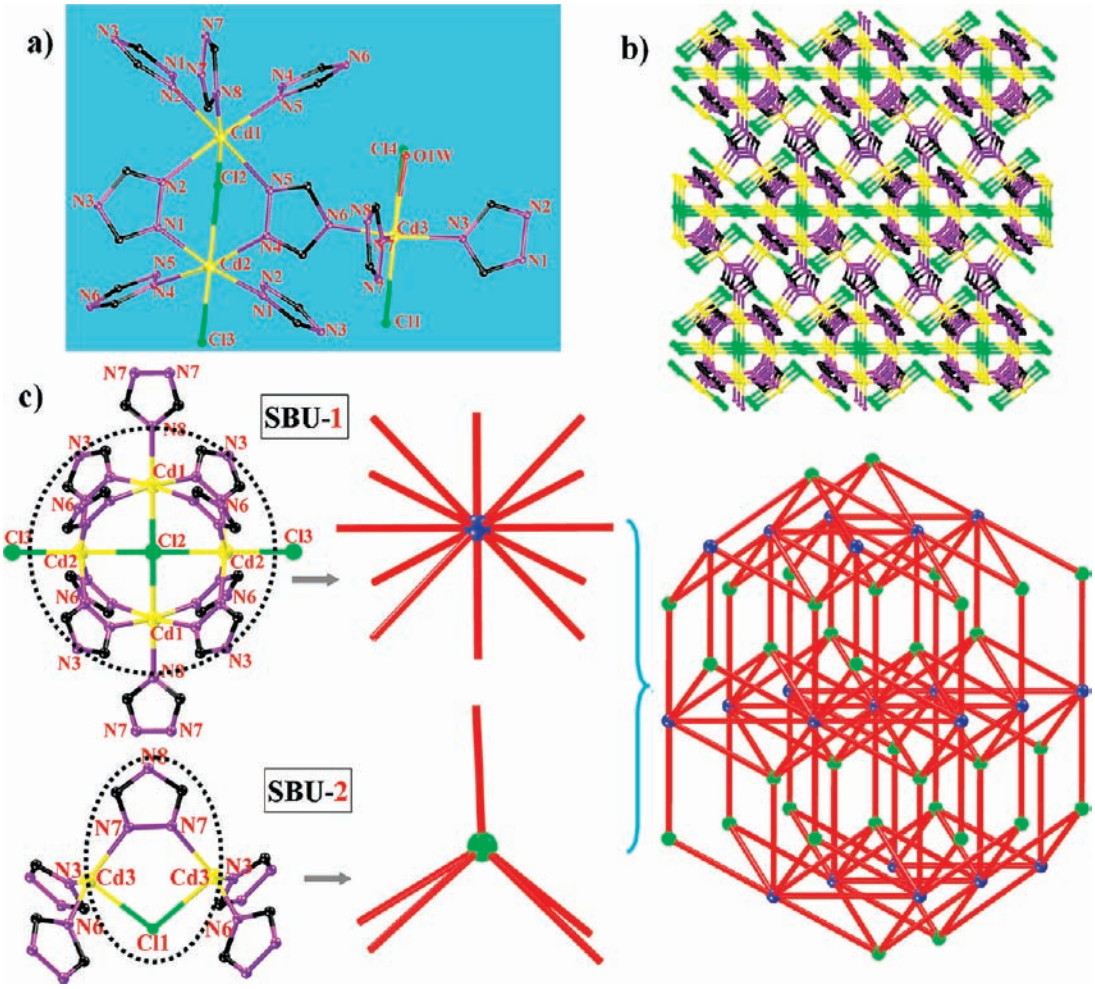

Figure 2. (a) View of the coordination environment of cadmium atoms in **2**. (b) Ball and stick representation of the 3-D structure of **2** along the *c*-axis. (c) Topological representation of the 3-D (5, 12)-connected network for **2**.

molecules, larger than 8.0 Å in [Zn(trz)F], and we found that the accessible porosity is resulting in a "free" volume of 45.0% in **1** as compared to 43.9% in [Zn(trz)F], which was calculated by PLATON.[13]

In complex $[Cd_4(trz)_5Cl_3(H_2O)]$ (**2**), three unique cadmium atoms present different coordination geometries, wherein Cd1 and Cd2 are situated at centers of distorted $\{N_5Cl_1\}$ and $\{N_4Cl_2\}$ octahedrons, respectively, and that Cd3 exhibits distorted $\{N_3ClO\}$ trigonal bipyramidal geometry, as shown in Figure 2a.

The 3-D structure of **2** can be accomplished by two kinds of second building units (SBUs) (left of Figure 2c). SBU-1 is a tetranuclear Cd(II) cluster $[Cd_4(trz)_8Cl]^-$, formed by two Cd1 and two Cd2, eight bridging $\mu_{1,2}$-trzs, and one bridging μ_4-Cl2 located in the center of the cluster. SBU-1 exhibits a centrosymmetric and unprecedentedly tetranuclear cluster in a ternary metal/trz/halide system.[7] Recently, a similar tetranuclear cluster consisting of $[Mn_4Cl]$ and tetrazolates was reported as the SBU of a microporous MOF which exhibited excellent adsorption properties for hydrogen gas, and the tetranuclear cluster was suggested to contribute to the increased electrostatic potential responsible for the strong binding and hydrogen storage properties.[14] Furthermore, the adjacent SBU-1 is connected together through μ_2-Cl3 to form a 1-D linear chain along the *c*-axis direction (Figure S1, Supporting Information). Alternatively, the binuclear unit $[Cd_2(trz)Cl]^{2+}$, named as SBU-2, is constructed by two Cd3, one $\mu_{1,2}$-trz, and one μ-Cl1. SBU-1 and SBU-2 are further bonded together by Cd1−N8, Cd2−Cl3, Cd3−N3, and Cd3−N6 to form a fascinating 3-D structure, as viewed in Figure 2b. To understand this 3-D framework clearly, SBU-1 and SBU-2 could be regarded as 12- and 5-connected nodes, respectively (middle of Figure 2c), and this 3-D framework can be rationalized as a rare binodal (5, 12)-connected topological net with Schläfli symbol of $(3^2\cdot4^8)$ $(3^8\cdot4^{28}\cdot5^{12}\cdot6^{17}\cdot8)$ (right of Figure 2c).[15]

Additionally, the framework voids have been occupied by THF and water molecules, disordered in the channels. If the lattice solvent molecules were omitted, then the total solvent accessible volume in the unit cell could attain 308.2 Å^3, accounting for 22.6% of the total unit volume as calculated.[13]

(13) Spek, A. L. *Acta Crystallogr., Sect. A: Found. Crystallogr.* **1990**, *46*, C34.

(14) (a) Dincă, M.; Dailly, A.; Liu, Y.; Brown, C. M.; Neumann, D. A.; Long, J. R. *J. Am. Chem. Soc.* **2006**, *128*, 16876–16883. (b) Dincă, M.; Long, J. R. *J. Am. Chem. Soc.* **2007**, *129*, 11172–11176. (c) Horike, S.; Dincă, M.; Tamaki, K.; Long, J. R. *J. Am. Chem. Soc.* **2008**, *130*, 5854–5855. (d) Dincă, M.; Dailly, A.; Tsay, C.; Long, J. R. *Inorg. Chem.* **2008**, *47*, 11–13.

(15) Ramsden, S. J.; Robins, V.; Hyde, S. T. *Acta Cryst. A* **2009**, *65*, 81–108.

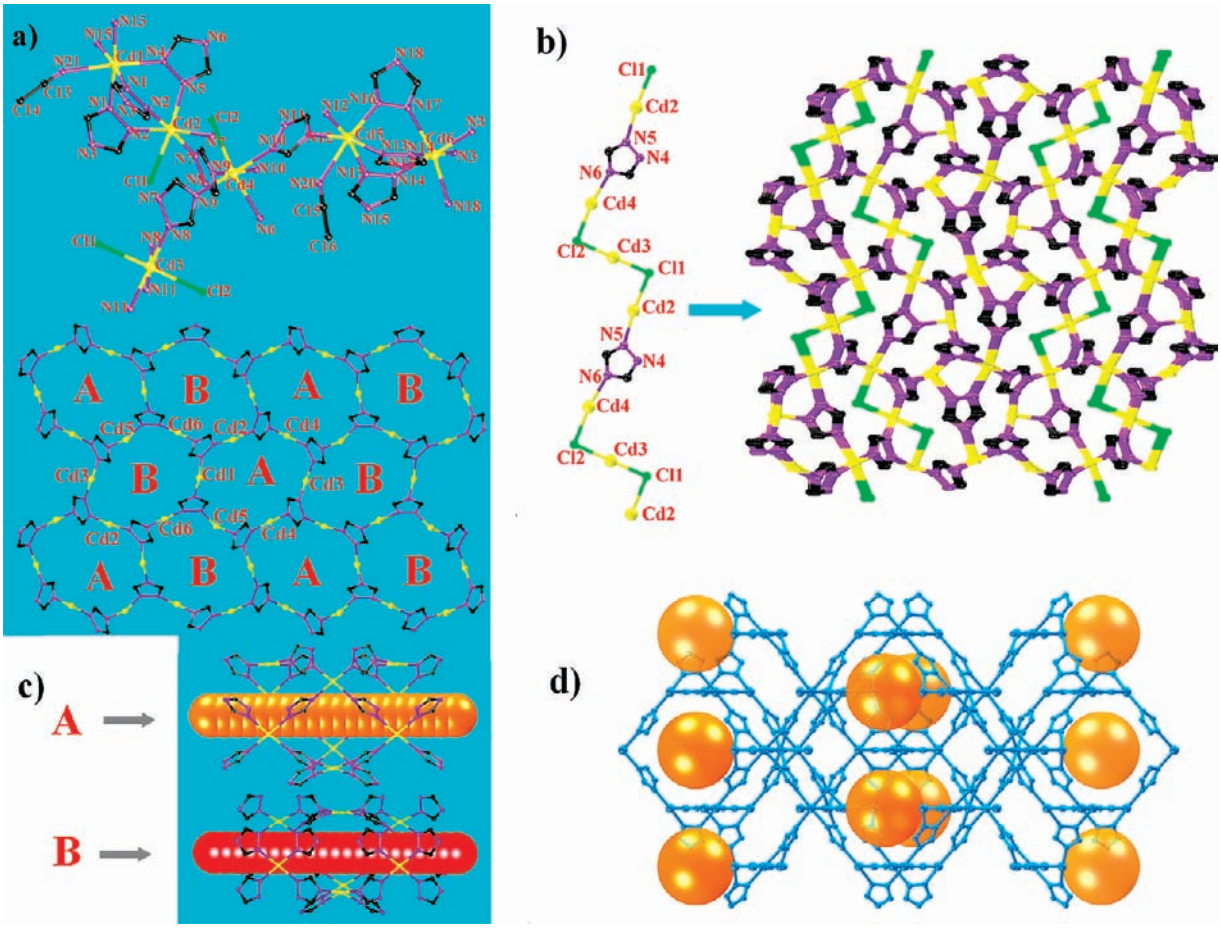

Figure 3. (a) Coordination environment of the cadmium atoms in **3**. (b) View of ball and stick representation of the 3-D structure of **3** in *bc*-plane. (c) View of the units of hexanuclear crown-like metallamacrocycles $[Cd_6(trz)_6]$ (top) and the open-ended nano channels of the types A and B along the *a*-axis (bottom). (d) The 3-D structure of **3**, showing the voids along the *c*-axis.

Single-crystal X-ray diffraction analysis reveals that there are six independent cadmium atoms in the asymmetric unit of $[Cd_3(trz)_2Cl(MeCN)]$ (**3**), wherein both Cd1 and Cd5 adopt distorted octahedral coordination geometry, with five nitrogen atoms from different trzs and one nitrogen atom from MeCN molecule. Cd2 and Cd4 are situated at the centers of two distorted $\{N_5Cl_1\}$ coordination octahedrons with five trz nitrogen atoms and one μ-Cl atom, respectively. Cd3 exhibits distorted $\{N_4Cl_2\}$ octahedral geometry with four trz nitrogen atoms and two independent μ-Cl atoms, and Cd6 is defined by six trz nitrogen atoms and displays typical octahedral geometry, as shown in Figure 3a.

The two independent μ-Cl atoms are bonded to Cd2−Cd4, cooperating with a $\mu_{2,4}$-bridged trz to give a 1-D zigzag chain which is embedded in the whole complex 3-D framework of **3** in two orientations while viewed along the *a*-axis (Figure 3b). If all of the μ-Cl atoms and μ_3-bridged trz ligands in the zigzag chains were artificially deleted, an interesting nanoporous framework including two similar kinds of 1-D nano channels would emerge (Figure 3c, up). These 1-D nano channels, regarded as "A" and "B" respectively, propagate infinitely in one direction parallel to the *a*-axis, which are wrapped like a cylinder and surrounded by each other, as shown in Figure 3c. Both of the open-ended channels possess windows comprised of hexanuclear crown-like metallamacrocycles $[Cd_6(trz)_6]$ in which A-$[Cd_6(trz)_6]$ contains Cd1−Cd5 generating the gold channel and B-$[Cd_6(trz)_6]$ consists of Cd1−Cd3, Cd5, and Cd6 forming the red channel, as shown in Figure 3c.[3d,6] The 3-D network of **3** accommodates coordinated MeCN molecules, which account for 22.6% solvent-accessible volume as determined from PLATON (Figure 3d).[13]

The crystal structure of $[Cd_3(trz)_4Cl_2]$ (**4**) exhibits two distinct kinds of cadmium sites in the asymmetric unit, as depicted in Figure 4a, wherein Cd1 presents an octahedral $\{CdN_4Cl_2\}$ site, defined by four trz nitrogen donors in the equatorial plane and two axial μ-Cl atoms, while Cd2 is based on trigonal bipyramidal geometry $\{CdN_4Cl\}$ and on five connected, respectively, by three equatorial trz nitrogen atoms as well as one trz nitrogen and one μ-Cl atom in the axial positions. The two bridging chlorine atoms in **4** have different bonding modes: Cl1 is bridged to two Cd1 showing μ_2-mode, and Cl2 is bridged to two Cd1 and one Cd2 showing μ_3-mode. Cd1 and all of the chlorine atoms build up 1-D zigzag chains in two orientations along the *b*-axis. Cd2 is linked to this chain through a Cd2−Cl2 bond just as terminal branches but not extending to a higher dimensional structure (Figure 4b).

When all of μ_3-bridged trzs are entered into the $[Cd_3Cl_2]_n^{4n+}$ chains, an interesting 3-D structure is generated which would keep its dimensionality in spite of the existence of chlorine atoms (Figure 4c). In other words,

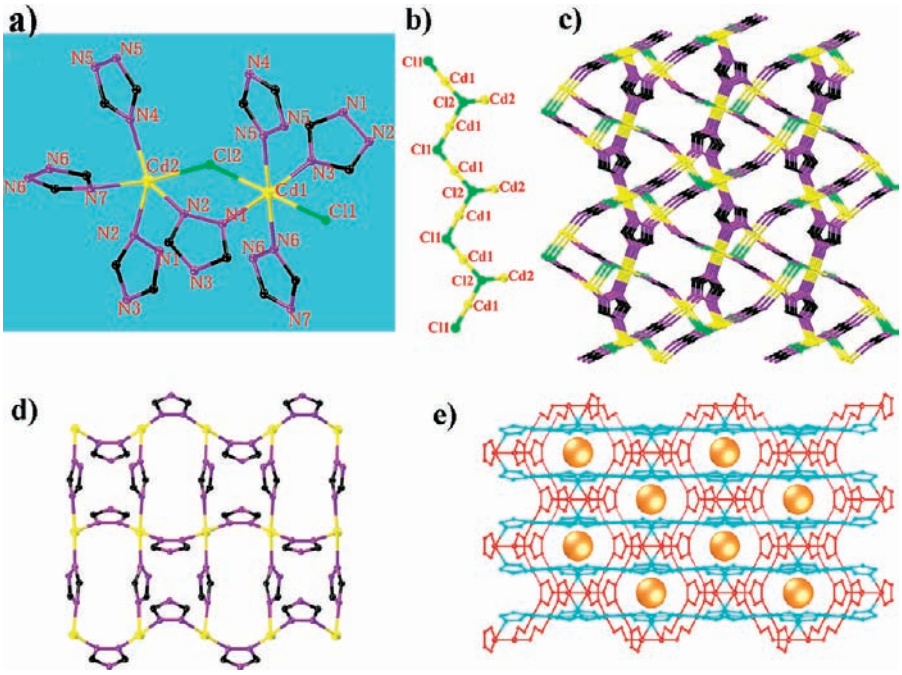

Figure 4. (a) Coordination environment of the cadmium atoms in **4**. (b) View of the 1-D Cd−Cl zigzag chain in complex **4**. (c) Ball and stick representation of the 3-D structure of **4** along the *b*-axis. (d) View of the $[Cd(trz)_2]_n$ layer of **4** in the *bc*-plane. (e) View of 3-D structure of **4** along the *a*-axis, showing the voids that contain the solvent molecules.

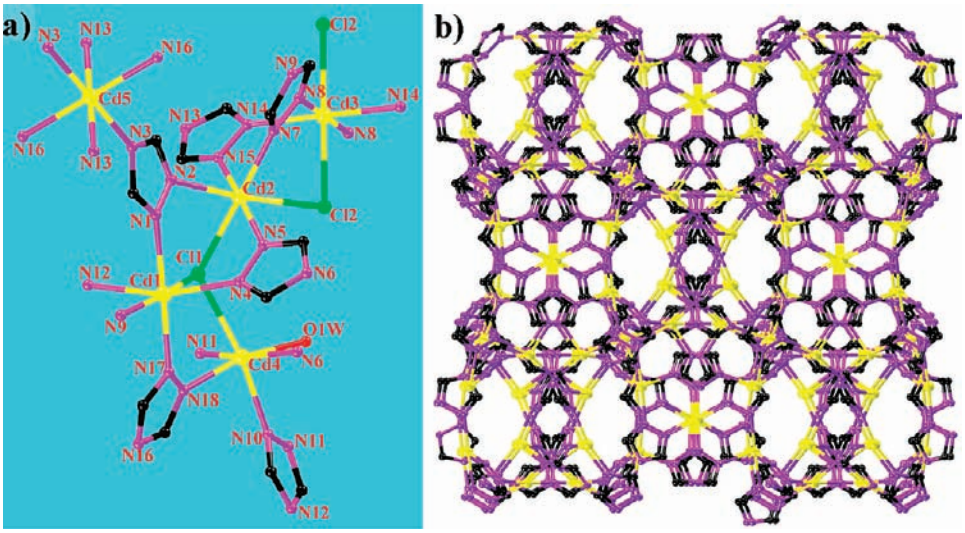

Figure 5. (a) View of the coordination environment of the cadmium atoms in **5**. (b) View of the 3-D structure of **5** along the *c*-axis.

all of the cadmium atoms and the triazolates in **4** may also construct a 3-D structure which could be decomposed into 2-D substructures and Cd2 atoms. The 2-D substructure is formed through Cd1 linking to two $\mu_{1,2}$- and two $\mu_{2,4}$-bridged trzs to give a $[Cd(trz)_2]_n$ layer with uniform (4, 4) topology in the *bc*-plane (Figure 4d). Then the third remaining N sites of these trzs are joined to Cd2 to give the 3-D structure which means that Cd2 atoms are located between two paralleling 2-D sheets by four Cd−N bonds for each one (Figure S2, Supporting Information). Furthermore, if we consider trz ligands as three-connected nodes and Cd1 and Cd2 as four-connected nodes, the 3-D framework exhibits a (3, 4)-connected trinodal net with Schläfli symbol of $(6^3)\cdot(6^2\cdot8^4)\cdot(6^2\cdot8^2\cdot10^2)$, as shown in Figure S3, Supporting Information.[15]

X-ray diffraction analysis reveals that 1-D channels can be observed running parallel to the *c*-axis in **4**; enclosed in the channels are free water molecules (Figure 4e). PLATON program analysis suggests that there is approximately 12.4% of the crystal volume occupied by solvent molecules.[13]

For complex $[Cd_4(trz)_6Cl_2(H_2O)_{0.5}]$ (**5**), there are five-independent cadmium atoms in the asymmetric unit displaying distinct octahedral coordination modes, as shown in Figure 5a. Cd1 is coordinated to five trz nitrogen atoms and one μ_3-Cl atom to form a $\{CdN_5Cl\}$ octahedral geometry. Cd2 and Cd3 show a similar coordination environment in which both cadmium atoms are bridged by two trzs and one μ-Cl atom with Cd···Cd distance of ca. 3.77 Å, then the other three coordination

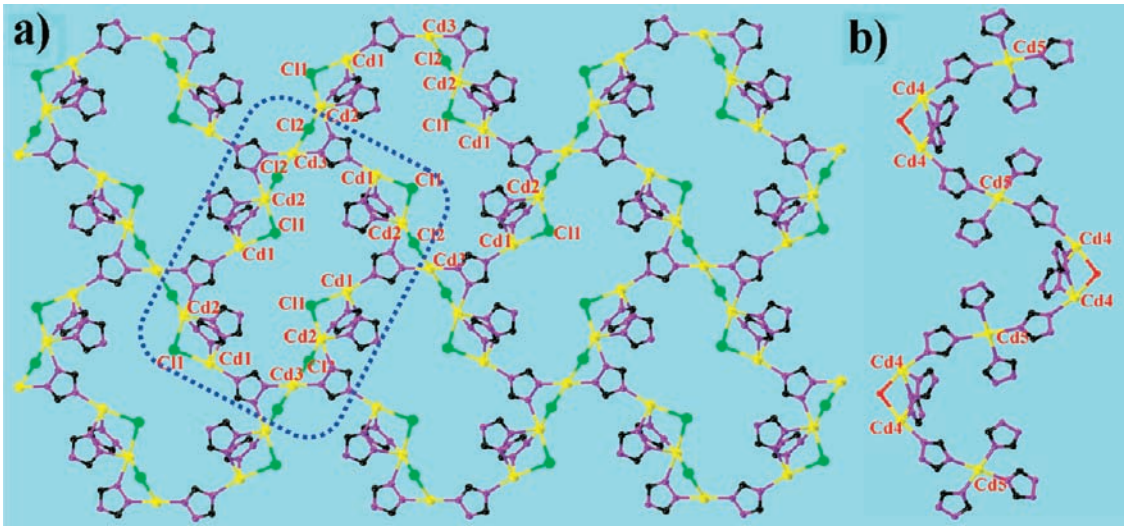

Figure 6. (a) View of the 2-D substructure of **5** in the *ab*-plane. (b) View of the S-shaped chain of **5**.

sites are occupied by two nitrogen atoms from trzs and one μ-Cl atom. The difference between the two coordination spheres is the arrangement of six donors wherein the two μ-Cl atoms are bonded to Cd2 in a cis form and Cd3 in a trans form. Cd4 presents an octahedral $\{CdN_4ClO\}$ site defined by three trz nitrogen donors and one μ_3-Cl atom in the equatorial plane and one trz nitrogen donor and one μ-bridged water oxygen atom in the axial positions. The last unique central atom Cd5 displays a uniquely perfect octahedral coordination sphere of $\{Cd(trz)_6\}$.

The crystallographically unique five Cd(II) centers, six triazolates, two chloride donors and half of a disordered coordination water molecule in **5** construct a particularly complicated 3-D microporous framework. To understand and simplify this complex 3-D structure in **5**, the whole network could be disassembled into two sets of substructures. The first substructure is a 2-D layer which consists of rectangle-like decanuclear $[Cd_{10}(trz)_{14}Cl_{10}]^{4-}$ metallacycles in two orientations, in which one macrocycle is surrounded by six others and the neighboring two macrocycles share part of an edge or a corner (Figure 6a). The second substructure is a 1-D S-shaped chain which is constructed by binuclear clusters $[Cd_2(trz)_2(\mu_2\text{-}H_2O)]^{2+}$ linked through coordination bonds of Cd5 and two $\mu_{2,4}$-bridged trzs, as shown in Figure 6b. The 2-D layers and 1-D S-shaped chains propagate interminably and then further interlink each other to form the final intricate 3-D framework of **5**.

In addition, approximately 13.4% of the framework voids have been occupied by disordered water molecules with a volume of about 726.0 Å^3 in each cell unit calculated from PLATON program.[13]

Thermogravimetric Analysis (TGA). As shown in Figure S5, Supporting Information, the thermal stabilities of these five complexes have already been performed on crystalline samples under a nitrogen atmosphere. The TGA curves show that all of these coordination frameworks are stable up to about 350 °C, and three stages of weight loss are observed in the temperature from 40 to 800 °C.

For all complexes, similar weight losses were observed in the temperature range of 50−350 °C. As shown in Figure S5, Supporting Information, the first weight loss of 6.02% for **1**·H_2O, 3.65% for **2**·1.25THF·2.5H_2O, 5.53% for **3**, 1.83% for **4**·0.5H_2O, and 5.06% for **5**·3.5H_2O shows that these preliminary degressive processes correspond to the loss of whole lattice water molecules except for compound **3** accommodating coordinated acetonitrile molecules (calcd 7.68, 4.28, 7.45, 1.32, and 5.98% for all complexes, respectively). For complexes **1**·H_2O, **2**·1.25THF·2.5H_2O, and **3**, the second weight loss in the temperature range of 350−450 °C was 26.24, 34.21, and 30.91%, in good agreement with the loss of triazolate ligands (calcd 28.23, 37.19, and 30.93%). The TG curve of complexes **4**·0.5H_2O and **5**·3.5H_2O exhibits a sharp weight loss in the temperature range 325−450 °C, corresponding to the weight loss of three trz ligands for **4**·0.5H_2O (exp. 27.80, calcd 29.91%) and one and a half trz ligands for complex **5**·3.5H_2O (exp. 9.71, calcd 9.58%). The third-step weight loss of all frameworks corresponds to the decomposition of organic components and chloride ions, respectively.

Photoluminescence Properties. The coordination polymeric systems usually display different optical properties as compared to the free ligands, such as fluorescent excitation/emission wavelength, intensity, lifetime, and so on. This provides an effective way to produce functional materials with desired properties. However, up to now, rational design and synthesis of desired coordination polymers is still a challenge. Recently, polymeric Cd(II) complexes have been intensively investigated for attractive fluorescence properties and potential applications as new luminescent materials, such as light-emitting diodes (LEDs).[16] Lu's, Yao's, and Zubieta's group has reported a series of Zn(II)/Cd(II) 1,2,4-triazolate polynuclear complexes and coordination polymers with strong blue fluorescence.[5,16] In this study, photoluminescent properties of these five coordination polymers have been explored at room temperature in the solid state, since all compounds are virtually insoluble in most common solvents, such as water, methanol, ethanol, and so on.

(16) (a) Zhang, Q.-C.; Liu, Y.; Bu, X.-H.; Wu, T.; Feng, P.-Y. *Angew. Chem., Int. Ed.* **2008**, *47*, 113–116. (b) Wang, M.-S.; Guo, S.-P.; Li, Y.; Cai, L.-Z.; Zou, J.-P.; Xu, G.; Zhou, W.-W.; Zheng, F.-K.; Guo, G.-C. *J. Am. Chem. Soc.* **2009**, *131*, 13572–13573.

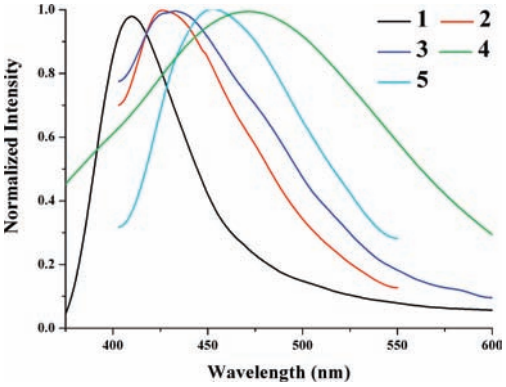

Figure 7. Emission spectra for all complexes (containing guest or lattice solvent molecules except for **1**) in the solid state at room temperature.

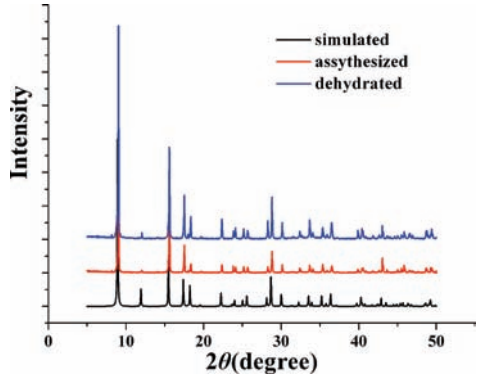

Figure 8. PXRD patterns of complex $\mathbf{1}\cdot H_2O$, simulated, as-synthesized, and dehydrated.

In these five as-synthesized complexes, four products with the exception of **1** containing guest or lattice solvent molecules display blue fluorescent emission bands respectively at 427, 434, 471, and 451 nm upon excitation at the same wavelength of 275 nm (Figure 7), which approachs the emission wavelength of 421 nm for the free 1,2,4-triazole ligand (Figure S6, Supporting Information).[5d] Though complex $\mathbf{1}\cdot H_2O$ fails to exhibit observable photoluminescence, interestingly, if it was dehydrated by drying at 160 °C in a high vacuum, a broad maximum emission peak at 410 nm would be observed (Figure 7). The powder X-ray diffraction patterns (PXRD) of **1** (Figure 8) have proved that the crystal lattice keeps the same when dehydrated. Furthermore, the luminescent quenching of $\mathbf{1}\cdot H_2O$ may be attributed to solvent molecules occupying the cavities of the 3-D framework, and the significant guest-responsive photoluminescence gives an opportunity for the potential application of this compound.

The emissions observed for materials of the Cd(II)/trz//Cl^- class maybe tentatively assigned as originating from intraligand $\pi-\pi^*$ transitions. In these complexes, the highest occupied molecular orbitals (HOMOs) are presumably associated with the π-bonding orbitals from aromatic 1,2,4-triazolate rings, whereas the lower unoccupied molecular orbitals (LUMOs) are associated mainly with the ligand π^* character rather than the Cd−Cl σ^*-antibonding orbitals, localized more on the metal centers. In our opinion, the photoluminescent emissions of these complexes are neither ligand-to-metal charge transfer (LMCT) nor metal-to-ligand charge transfer (MLCT) in nature, and maybe assigned to ligand-to-ligand charge transfer (LLCT), which is in reasonable agreement with literature examples on this class of zinc coordination polymers previously reported by Xiong et al.[17] It implied that the complexities of the 3-D structures in this study have little influence on their photoluminescence properties, and the red-shifts of their emission bands compared to the free ligand could be ascribed to the reduction of the HOMO−LUMO gap caused by the ligand deprotonation.

Conclusions

We have reported here the study on the ternary Cd(II)/trz/Cl^- system which behaves relatively as fixed components as compared to other reported bivalent metal triazolates with different metal ions and/or various inorganic anions. The successful combination of these three contributions depends on a higher solvothermal temperature and a weak basic reaction medium; in which conditions, five ternary coordination polymers have been produced. Interestingly, they have distinct stoichiometric ratios of ternary components that generates their versatile 3-D frameworks.

On the basis of structural investigations, it was found that all triazolates in these five coordination polymers display a $\mu_{1,2,4}$-bridging fashion linking to three cadmium atoms at the same time, whereas chloride ions give various coordination modes, including μ_2-, μ_3-, and even μ_4-bridging. Additionally, the third ternary component cadmium atoms present octahedral and trigonal bipyramidal coordination geometries with the absence of a tetrahedral coordination sphere in this study, which results in dissimilar structural modes as compared to Zn(II) analogies.[5] Though the 3-D frameworks of these five coordination polymers are constructed by very distinct substructures, for example, clusters, rings, chains, and even 2-D layers, as shown in Table 2, the dinuclear cadmium cluster is the common structural subunit extensively existing in all of these structures, which may present as $[Cd_2(trz)Cl]^{2+}$, $[Cd_2(trz)_2Cl]^+$, or $[Cd_2(trz)_3]^+$. These dinuclear clusters acted as elementary SBUs joined together to generate a chain-like subunit, such as in the structure of **1** and **5**, or to build up larger cluster SBUs, such as tetranuclear cluster $[Cd_4(trz)_8Cl]^-$ in **2**. How to control the assembly of these dinuclear clusters to give desired frameworks is still a challenge.

All of five complexes display intense blue-fluorescent emissions except for **1**, which exhibits photoluminescence only in the absence of guest molecules. This phenomenon implies that **1** could be used as a potential guest-responsive photoluminescent material. On the basis of this work, we will pursue our research by replacing cadmium with other metals and/or using unsymmetrical triazole ligands to synthesize novel coordination polymers and to study their fascinating properties.

Acknowledgment. This work was supported by the NSFC (no. 20801034) and NSF of Guangdong Province (no. 8251503101000001 and 06027203).

Supporting Information Available: X-ray crystallographic data in CIF format, TGA curves, and PXRD as well as excitation and emission spectra for 1,2,4-triazole. This material is available free of charge via the Internet at http://pubs.acs.org.

(17) (a) Wang, X.-S.; Tang, Y.-Z.; Huang, X.-F.; Qu, Z.-R.; Che, C.-M.; Chan, P. W. H.; Xiong, R.-G. *Inorg. Chem.* **2005**, *44*, 5278–5285. (b) Zhai, Q.-G.; Wu, X.-Y.; Chen, S.-M.; Zhao, Z.-G.; Lu, C.-Z. *Inorg. Chem.* **2007**, *46*, 5046–5058.